Jensen, T. T., Potticary, J., Terry, L. R., Bruce Macdonald, H. E., Brandenburg, J. G., & Hall, S. R. (2017). Polymorphism in crystals of bis(4-bromophenyl)fumaronitrile through vapour phase growth. *CrystEngComm*, *19*(48), 7223-7228. https://doi.org/10.1039/c7ce01543g

Supplementary Information for Polymorphism in crystals of bis(4-bromophenyl)fumaronitrile through vapour phase growth

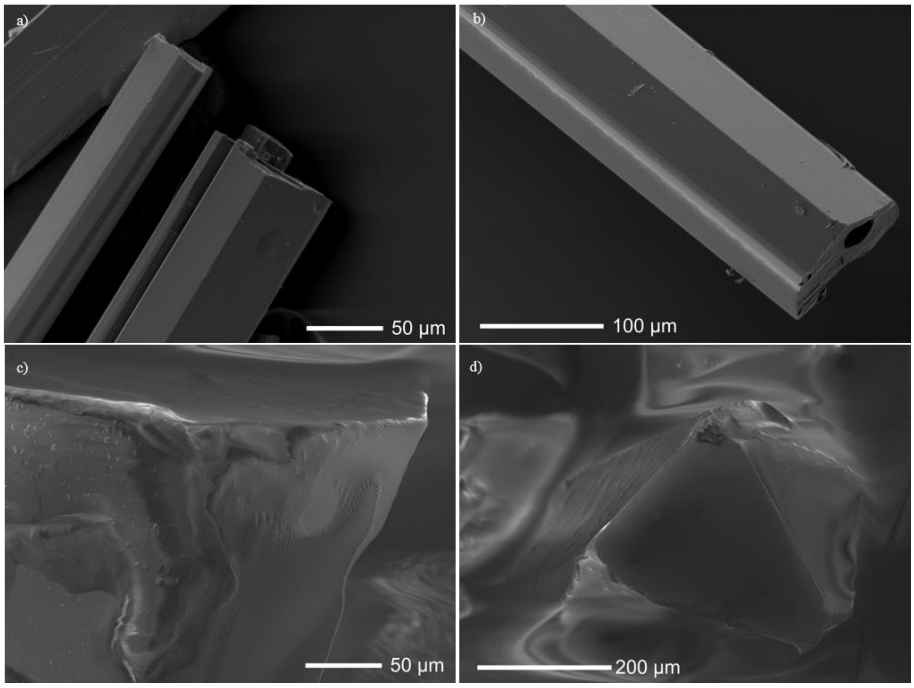

Fig. S1 SEM images of a) and b) form 2 crystals grown via physical vapour transport; c) and d) form 1 crystals grown from solution.

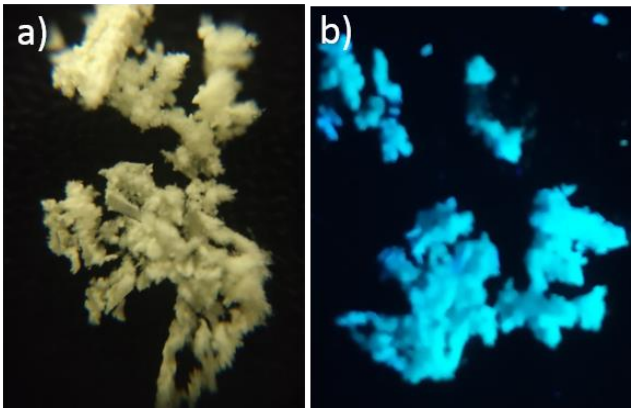

Fig. S2 Pictures of powder from vacuum sublimation a) under lab light and b) under 365 nm UV light.

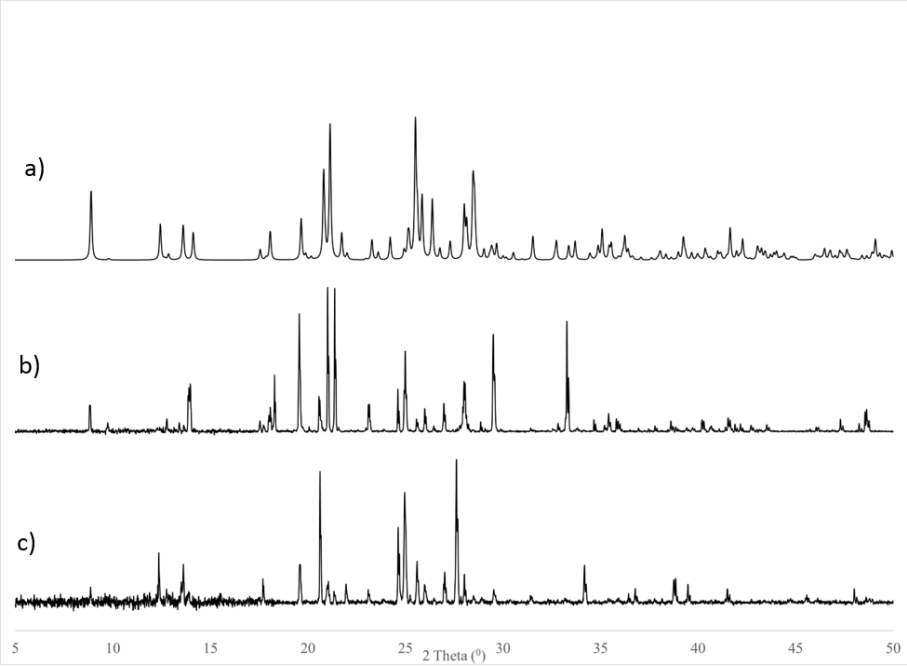

Fig. S3 pXRD patterns of (a) Br-FN form 1, calculated from SC-XRD data. (b) and (c) pXRD patterns of white powder and needles extracted from the PVT growth tube, respectively, indicating that both are of form 1. Discrepancies between peak intensities arise due to preferred orientation of crystals on the sample holder.

Formatted: Centered

Formatted: Font: 11 pt

Formatted: Justified

Formatted: Font: Bold, No underline

Formatted: No underline

~~**Fig. S2** pXRD patterns of (a) Br-FN form 1, calculated from SC-XRD data. (b) and (c) pXRD patterns of white powder and needles extracted from the PVT growth tube, respectively.~~

Fig. S4 pXRD patterns of (a) Br-FN form 2, calculated from SC-XRD data. (b) pXRD pattern of white powder from vacuum sublimation, indicating that it is of form 2. Discrepancies between peak intensities arise due to preferred orientation of crystals on the sample holder.

Formatted: Centered

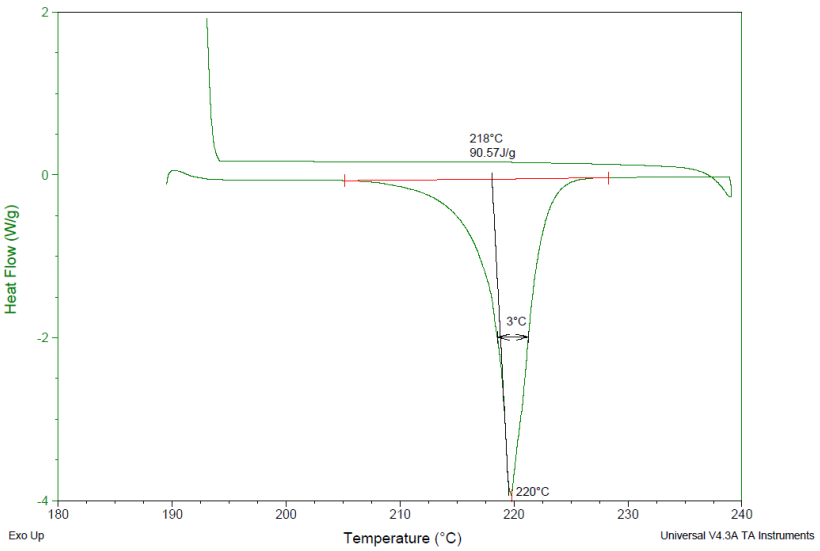

Fig. S~~3~~ Differential scanning calorimetry measurements of Br-FN form 1, displaying a measured melting point of 220 ^{0}C.

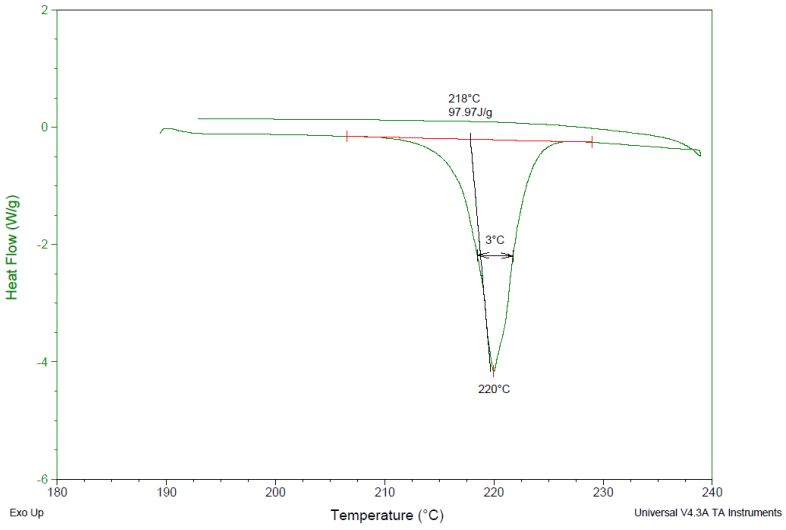

Fig. S~~4~~ Differential scanning calorimetry measurements of Br-FN form 2, displaying a measured melting point of 220 ^{0}C.

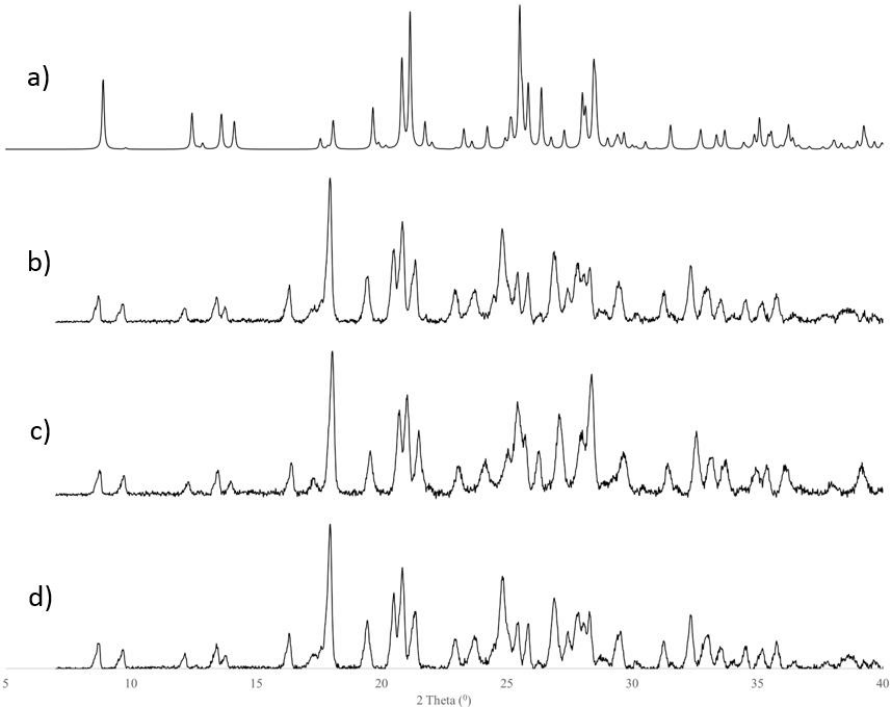

Fig. S~~7~~5 XRD patterns of (a) Br-FN form 1, calculated from SC-XRD data; (b) Br-FN form 1 powder taken at 300K before cooling; (c) at 12 K and (d) after heating back to 300K. These results show that no phase change occurs in crystals of form 1 over the temperature ramp. The differences in peak intensity from c) to b) and d) are likely due to contraction of the unit cell at low temperature.

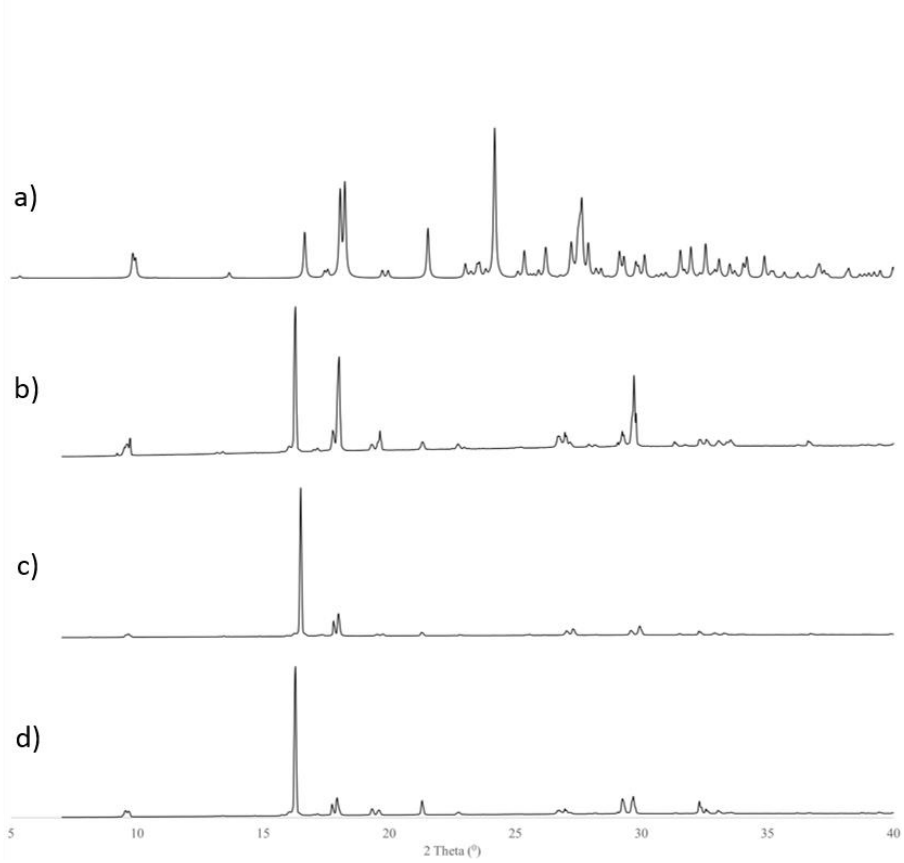

Fig. S~~6~~ XRD patterns of (a) Br-FN form 2, calculated from SC-XRD data; (b) Br-FN form 2 powder taken at 300K before cooling; (c) at 12 K and (d) after heating back to 300K. These results show that no phase change occurs in crystals of form 2 over the temperature ramp. The differences in peak intensity from d) to b) and c) are likely due to shattering of crystallites as they are cooled and heated.

	Form 1	**Form 2**
Empirical formula	$C_{16}H_8N_2Br_2$	$C_{16}H_8Br_2N_2$
Formula weight	388.06	388.06
Temperature/K	100(2)	100(2)
Crystal system	triclinic	triclinic
Space group	*P*-1	*P*-1
***a*/Å**	7.8318(2)	3.8726(1)
***b*/Å**	9.3958(3)	10.7671(4)
***c*/Å**	10.5371(3)	16.5188(6)
α/°	87.814(2)	90.217(3)
β/°	70.834(1)	93.186(3)
γ/°	74.150(2)	98.738(2)
Volume/Å^3	703.43(4)	679.68(4)
Z	2	2
ρ_{calc}g/cm^3	1.832	1.896
μ/mm^{-1}	5.751	5.952
F(000)	376.0	376.0
Crystal size/mm^3	0.536 × 0.288 × 0.265	0.43 × 0.404 × 0.198
Radiation	MoKα (λ = 0.71073)	MoKα (λ = 0.71073)
2θ range for data collection/°	4.514 to 55.204	2.47 to 55.762
Index ranges	-10 ≤ h ≤ 9, -12 ≤ k ≤ 12, -13 ≤ l ≤ 13	-4 ≤ h ≤ 5, -14 ≤ k ≤ 14, -21 ≤ l ≤ 21
Reflections collected	12529	11146
R_{int} / R_{sigma}	0.0177 / 0.0153	0.0277 / 0.0275
Data/restraints/parameters	3262/0/181	3207/0/181
Goodness-of-fit on F^2	1.065	1.209
Final R indexes [I>=2σ (I)]	R_1 = 0.0161, wR_2 = 0.0404	R_1 = 0.0365, wR_2 = 0.0902
Final R indexes [all data]	R_1 = 0.0188, wR_2 = 0.0412	R_1 = 0.0420, wR_2 = 0.0918
Largest diff. peak/hole / e Å^{-3}	0.39/-0.26	1.30/-0.86

Table S1 Crystal data and structure refinement for form 1 and 2.

Additional details on DFT calculations:
Full relaxation of the crystals (including unit cell parameters) at the HSE-3c electronic structure level decreased the unit cell volume by 5 and 3% for form 1 and form 2, respectively, compared to the experimentally measured one at 100 K. The structural details are summarized in Table S2.

	Form 1	**Form 2**
Crystal system	Triclinic	Triclinic
Space group	P -1	P -1
a/Å	7.6605	3.7759
b/Å	9.5059	10.7357
c/Å	10.4055	16.6081
α/ Å	92.568	90.089
β/°	108.391	90.012
γ/°	73.840	100.170
Volume/Å^3	689.85	662.67
Z	2	2
Temperature/ K	0	0

Table S2 Unit cell parameters of form 1 and form 2 from HSE-3c optimizations.

The computed HSE-3c lattice energy (with experimental cell parameters) is -148.3 kJ/mol for form 1 and -151.3 kJ/mol for form 2. This was confirmed by PBE-D3[1,2] single-point energies on the HSE-3c structures, evaluated in a projector augmented plane wave basis set with energy cutoff of 800eV with the VASP 5.4 code.[3] Relaxation of the unit cell at the HSE-3c level changed the computed lattice energies only slightly to -149.5 kJ/mol and -153.4 kJ/mol.

References

1 J. P. Perdew, K. Burke and M. Ernzerhof, *Phys. Rev. Lett.*, 1996, **77**, 3865–3868.

2 S. Grimme, J. Antony, S. Ehrlich and H. Krieg, *J. Chem. Phys.*, 2010, **132**, 154104.

3 G. Kresse and J. Furthmüller, *Comput. Mater. Sci.*, 1996, **6**, 15–50.